Research Article   **Open Access**

S. Omar, J. Pastore, A. Bouchet, S. Pellice, V. Ballarín, S. Ceré, and J. Ballarre*

SiO$_2$-CaO-P$_2$O$_5$ (58S) sol gel glass applied onto surgical grade stainless steel by spray technique: morphological characterization by digital image processing

Abstract: AISI 316L stainless steel is commonly used as a low-cost material for permanent implants. It can be protected for degradation and corrosion by applying a hybrid silica based coating. Also the bioactive response of the implant can only be achieved by functionalizing the coated implant surface. The aim of this work is to synthesize and characterize a sol-gel made glass particles from the system SiO$_2$-CaO-P$_2$O$_5$ with potential as bone inductive material, with and without an aging treatment of the precursor solution. The glass was synthesized by sol-gel technique that, comparing with melt glasses, generates an open net structure that could lead to particle dissolution and apatite deposition for biological purposes. The synthesized glass is dispersed by spray onto AISI 316L protected by a hybrid silica based coating, generating deposits with different size and morphology. To characterize the particles composition, microRaman spectroscopy was applied. It showed that no significant changes were reached after aging or thermal treatment of the deposited particles. Image processing techniques based on Mathematical Morphology were used to analyze morphology and sizes of the deposits obtain with the different sols (aged and no aged). Aproximately 50% of the surface was covered with particles made with a glass aged, and a 25% of covered area

was reached with no aged one. When no aged glass particles were deposited, the particle size distribution shows the presence of many big particles with a roundness factor between 0.8 and 1 in a high percentage, meaning that they are spherical due to the presence of solvent and with a more open glass structure in the no aged glass. The Digital Image Processing and Raman spectroscopy tools help to analyze, characterize and quantify the bioactive particles deposited onto coated surgical grade stainless steel in terms of morphology, distribution and composition.

Keywords: 58S glass; Stainless steel; Coatings; Spray deposition; Image analysis; Mathematical morphology

1 Introduction

The use of metals for biotechnological applications is limited not only by the specific function they have to assure but also the selective media where they are placed, resulting corrosive protection an essential task. Also the bioactivation of a surface that per se is not biologically active is important for a medical function. One example is the protection and functionalization of AISI 316L for orthopaedic implants, since the media is extremely aggressive and can lead to undesirable chemical reactions of the surface with the living tissues.

There are many techniques to improve material's surface. The application of a protective coating becomes a promising choice, as it generates a new surface which will interact with the surrounding media acting as a barrier for ions migration. In matter of coatings, the organic-inorganic hybrid sol gel made materials have taken the attention from academics and technological institutes due to the unusual combination of physical and chemical properties which are capable to exhibit [1, 2]. The family of greatest potential for development is derived from the hydrolytic condensation products of functionalized alkoxysi-

S. Omar, S. Pellice, S. Ceré: Material's Science and Technology Research Institute. INTEMA - Universidad Nacional de Mar del Plata (UNMdP), Juan B. Justo 4302, Mar del Plata, Argentina; National Research Council (CONICET)
J. Pastore, A. Bouchet: National Research Council (CONICET);
V. Balların: Digital Image Processing Lab. ICyTE. Universidad Nacional de Mar del Plata (UNMdP)
*Corresponding Author: J. Ballarre: Material's Science and Technology Research Institute. INTEMA - Universidad Nacional de Mar del Plata (UNMdP), Juan B. Justo 4302, Mar del Plata, Argentina; National Research Council (CONICET); Email: jballarre@fi.mdp.edu.ar; Tel.: +54 223 481 6600; Fax: +54 223 481 0046

lanes pure or enriched with tetraethoxysilane (TEOS) [3–5]. The final hybrid material consists in a Si-O-Si network modified with some organic groups. The traditional way to apply this kind of hybrid coating is by dipping, as this technique gives homogeneous and crack free coatings with excellent corrosive properties.

Even though a hybrid sol-gel coating can improve corrosive behavior, osseointegration cannot take place between materials which show no signs of bioactivity and here another strategy requires to be chosen. As bioactive glasses have the ability to bond with living tissues forming an apatite layer, they qualify as an alternative. If they are made by sol-gel, they have also the advantage of high degree of purity and good homogeneity [6]. At this point, the use of a known bioactive glass (58S) made by the sol-gel route becomes an interesting issue. This consists in a chemistry-based synthesis where a solution containing the compositional precursors undergoes polymer type reactions at room temperature to form a gel. Precursors of SiO_2 and P_2O_5 are usually alkoxides due to their availability, whereas inorganic salts are generally used to generate the calcium component [6]. After hydrolysis and polycondensation that take place at room temperature, a gel is obtained which can be aged, dried and stabilized at different conditions [7]. Once obtained the gel, a drying process and a thermal treatment results essential to consolidate it, and also to remove by-products of the non-alkoxide precursors [8]. With different aging treatments, it is thought to obtain different shrinkages of the structure, and so different dissolution rate of the glass.

In this work, we propose to apply 58S glass made by sol gel technique in a sol condition, deposited by spray method with the aim of generating bioactive particles or dots over a protected AISI 316L stainless steel. The spray deposition of the bioactive glass is expected to follow certain distribution, covering some surface's percentage and having a specific shape. These last named aspects, need to be studied as they affect the performance of the whole system. Digital Image Processing (DIP) helps to this analysis. Mathematical Morphology will allow to segment and characterize the deposited particles.

One of the most important tasks in Biomedical Image Processing is the segmentation, regarded as the ability to detect objects, with some specific features, in the image. This stage is of great importance for any automatic vision system, since it is the first processing stage. It affects severely the late stages of interpretation, providing useful information, like regions and/or edges. Mathematical Morphology (MM) has been successfully used as a tool in image segmentation. The MM is a theory based on concepts of geometry, algebra, topology and set theory. The main objective of the MM is to extract information of the geometry and topology of an unknown set present in an image. The "structuring element" (SE) is a set completely defined with a known geometry, which is compared with the whole image through logical operations [9]. The shape and size of the structuring element allow to quantify if the SE is contained in the image or not.

The aim of this work is to synthesize, deposit and characterize a sol-gel made glass with potential as bone inductive material, with and without an aging treatment of the gel glass. The generated glass is dispersed by spray deposition onto surgical grade stainless steel protected by a hybrid silica based coating, generating deposits with different morphology. Spectroscopic and Digital Image Processing tools are used to characterize these systems.

2 Materials and methods

2.1 Substrates

Stainless steel AISI 316L (SS) was used as base material. A protective sol-gel silica based coating (TMS) was applied onto the steel. The hybrid organic-inorganic sol to produce the TMS coating was prepared with tetraethoxysilane (TEOS, 99% Sigma Aldrich), and methyltriethoxysilane (MTES, 98% Sigma Aldrich) and colloidal silica suspended in water (SiO_2, LUDOX 40 wt%, Dow). The molar ratio of the alkoxide was kept constant (TEOS/MTES = 40/60) and the addition of colloidal silica was 10 per cent in moles respect with the total amount of SiO_2. The final silica concentration was 200 g/L and the water amount was kept stoichiometric. This synthesis was performed in acidic catalysis with nitric acid (65% w/w, Merck).

Metallic cleaned and degreased steel substrates were covered with the TMS sol by dip-coating method with a extraction rate of 20 cm/min. A thermal treatment at $450°C$ for 30 minutes was carried out to consolidate the coating.

2.2 Glass synthesis and deposition

The 58S sol-gel glass (60 mol%. SiO_2, 36 mol.% CaO, 4 mol%. P_2O_5) was prepared using as precursors tetraethoxysilane (TEOS, 99% Sigma Aldrich), triethyl phosphate (TEP, 99% Sigma Aldrich) and calcium nitrate tetrahydrate ($Ca(NO_3)_2 \cdot 4H_2O$, Biopack), with a volume ratio of H_2O/HNO_3 (in vol) = 6. The nitric acid concentration was 65% w/w. The chosen method to generate bioactive spots over the new substrate (SS+TMS) was spray, fixing

the deposition parameters in 400 mm/s of speed rate, 23 cm distance between the spray gun and the target and a pressure which varied depending if the sol was or was not aged.

Half of the prepared sol was immediately applied by spray method (pressure: 0.8 Bar) onto the SS-TMS substrates and sintered in an electric oven at 70°C for 3 days. Gelation was observed to occur within a few hours at this temperature.

The other half sol was kept for a 24 hours aging process at room temperature in a tight container, before being applied by spray technique (pressure: 1 bar) on separate SS-TMS substrates and then dried at 70°C in the oven for 3 days.

Finally, two types of samples (SS-TMS substrates with the sprayed 58S glass with and without the aging treatment) were obtained. Half of each type were thermally treated in an oven at 450°C during 3 hours in order to eliminate nitrates and to allow calcium to diffuse into the silica network. The other half was dried at room temperature and stored until characterization was done.

After all of the procedure, four kinds of samples (all applied onto the same kind of substrate: SS+TMS) were obtained, where the 58S glass particles were generated in situ. Notation is summarized in Table 1.

Table 1: Different types of bioactive particles synthesized.

Sample name	Aging	Drying	Thermal treatment
58S		72 hs at 70°C in air	
58S_TT		72 hs at 70°C in air	3 hs at 450°C in air
58S_AG	24 hs closed at RT	72 hs at 70°C in air	
58S_AG_TT	24 hs closed at RT	72 hs at 70°C in air	3 hs at 450°C in air

2.3 Deposits characterization

2.3.1 Glass composition and structure

Raman spectroscopy was employed to characterize the chemical structure at a molecular bonding grade of the different glass particles deposited. This method provides information about the covalent bonds and vibrational modes of the molecules and compounds present in the

system. The equipment used was an inVia spectrometer (Renishaw, UK) system equipped with charge-coupled device (CCD) detector of 1040 × 256 pixels and coupled to a Leica microscope (DM-2500 model) (50×, 0.75 NA) with a computer-controlled x-y-z stage. A diode laser line (785 nm) was used as excitation source in combination with a grating of 1200 grooves/mm. The laser power was kept below 10% to avoid sample damage, employing one 10-sec acquisition for each data point. The spectral resolution was 4 cm^{-1}, and the spectra were taken from 100 to 1400 cm^{-1}.

2.3.2 Digital Image Processing

The basic morphological operators of the MM are erosion and dilation. Morphological erosion and dilation of the image by the structuring element are defined, respectively, as [10, 11]:

$$\varepsilon\,(f,b)\,(s,t) = \min\left\{f(s+x,t+y) - b(x,y)/\,(s \quad (1)\right.$$
$$\left. +x,t+y) \in D_f;\,(x,y) \in D_b\right\}$$

$$\delta\,(f,b)\,(s,t) = \max\left\{f(s-x,t-y) + b(x,y)/\,(s \quad (2)\right.$$
$$\left. -x,t-y) \in D_f;\,(x,y) \in D_b\right\}$$

where D_f and D_b are the domains of the functions f and b respectively.

Based on the combination of the previous operators, opening and closing can be defined as follows:

$$\gamma_b(f) = \delta_b\left(\varepsilon_b(f)\right) \quad (3)$$

$$\Phi_b(f) = \varepsilon_b\left(\delta_b(f)\right) \quad (4)$$

The opening is useful to remove small bright details smaller compared to the size and shape of the structuring element, the rest of the image is not modified. When filtering, in the step of erosion, a bright area surrounded by dark one is reduced. Particularly, if the size of the structuring element is greater than the bright area, this bright area totally disappears. Then, in the step of dilation, a bright area surrounded by dark one is expanded and therefore the image recovers its current shape, except of the details removed by erosion in the previous step. Similarly, the closure is useful to remove small dark details compared to the size and shape of structuring element, the rest of the image is not modified. The resulting image depends on the grey level, shape and size of the structuring element. Top-hat transform is a well-known and commonly used morphological technique for extracting locally bright or dark

objects from a grey scale image. Figure 1 shows an opening Top-Hat transform, which emphasizes locally bright objects that have been eliminated from the image by an opening filter. A structuring element larger than the structures to be filtered was used.

This transform is defined as the residual between the identity and a morphological opening [10, 11]:

$$\rho_b(f) = f - \gamma_b(f) \tag{5}$$

Since this transform emphasizes bright objects on a non-uniform background (See Figure 1), it is suitable for segmentation of the sol gel glass cover area by spray technique.
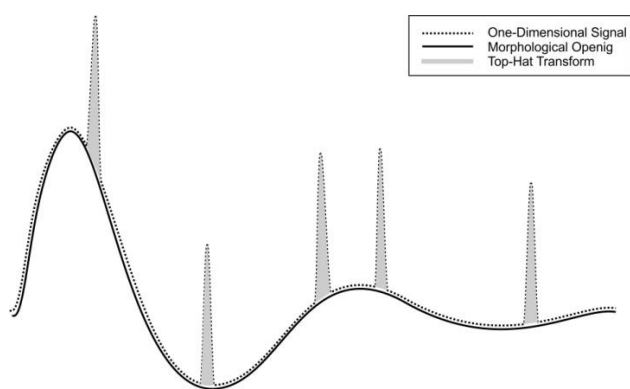

Figure 1: Top-Hat transform on a one-dimensional signal.

In order to characterize the structure of the glass particles we propose to segment the glass particles computing the opening Top-Hat transform, and binarizing the image.

Figure 2 shows the two steps of the proposed segmentation algorithm. First, particles were enhanced by an opening Top-Hat transform. Figure 2(b) shows the result grey-scale image where the enhanced regions representing particles. This image has a bimodal histogram which allows determining a threshold value to discriminate the particles from the background. Consequently a binary image is obtained, applying the automatic Otsu threshold algorithm [12], as it can be seen in Figure 2(c). In the following section we characterize glass deposition particles using a granulometric size distribution and shape factors from the binary image obtained in the previous step.

2.3.3 Morphological characterization by image processing

After segmentation of the sol gel glass deposited particles, the cover area, particle size and their distribution should be analyzed to complete the particles characterization. To calculate the granulometric size distribution (GSD), the following algorithm was proposed [11]:

$$G(\lambda) = 1 - \frac{\Omega(\lambda)}{\Omega(1)} \quad \lambda = 1, 2 \dots \tag{6}$$

where $\Omega(\lambda)$ represents the area of the opened image by a SE of the size $E_\lambda \left(\gamma_{E_\lambda}(f) \right)$, and $\Omega(1)$ the area under the original image. $\Omega(\lambda)$ is a discrete cumulative function, as far as it is monotonic. This function represents the variation of the area of the resulting image in each iteration of the opening.

Most traditional shape factors are mere combinations of size parameters (area, perimeter and diameter) normalized [13]. Table 2 lists the most used shape factors. Each of these parameters gives a different aspect of the shape.

Table 2: Shape factors.

Shape factors	Reference
$F = \frac{4\pi A}{P^2}$	Shape Factor
$R = \frac{4A}{\pi D_{\max}^2}$	Roundness
$R_a = \frac{D_{\max}}{D_{\min}}$	Aspect relationship
$E = \frac{l_f}{a_f}$	Elongation
$C = \frac{P_c}{P}$	Convexity

where:

A = area enclosed by the contour;

D_{min}/D_{max} = minimum/maximum diagonal of the area enclosed by the contour;

l_f = fiber length: defined as the length along the axis of the curvilinear shape;

a_f = maximum width of the curvilinear shape;

P = perimeter;

P_c = convex perimeter: defined as the length of a convex line circumscribing the object to be measured.

3 Results

Raman spectroscopy essays were made to analyze the effect of thermal treatment to the gel-glass evolution, Figure 3 shows Raman spectra of the 58S sol gel glasses with and without aging treatment (58S and 58S_AG) and with or without thermal treatment (58S_TT and 58S_AG_TT). The detailed position of the bands, are shown in Table 3.

With the aim of comparing the results obtained from the digital image processing, two systems are presented in Figure 4. Fig. 4(a) shows an optical microscopy of the 58S_TT coated sample and (b) shows the 58S_AG_TT one.
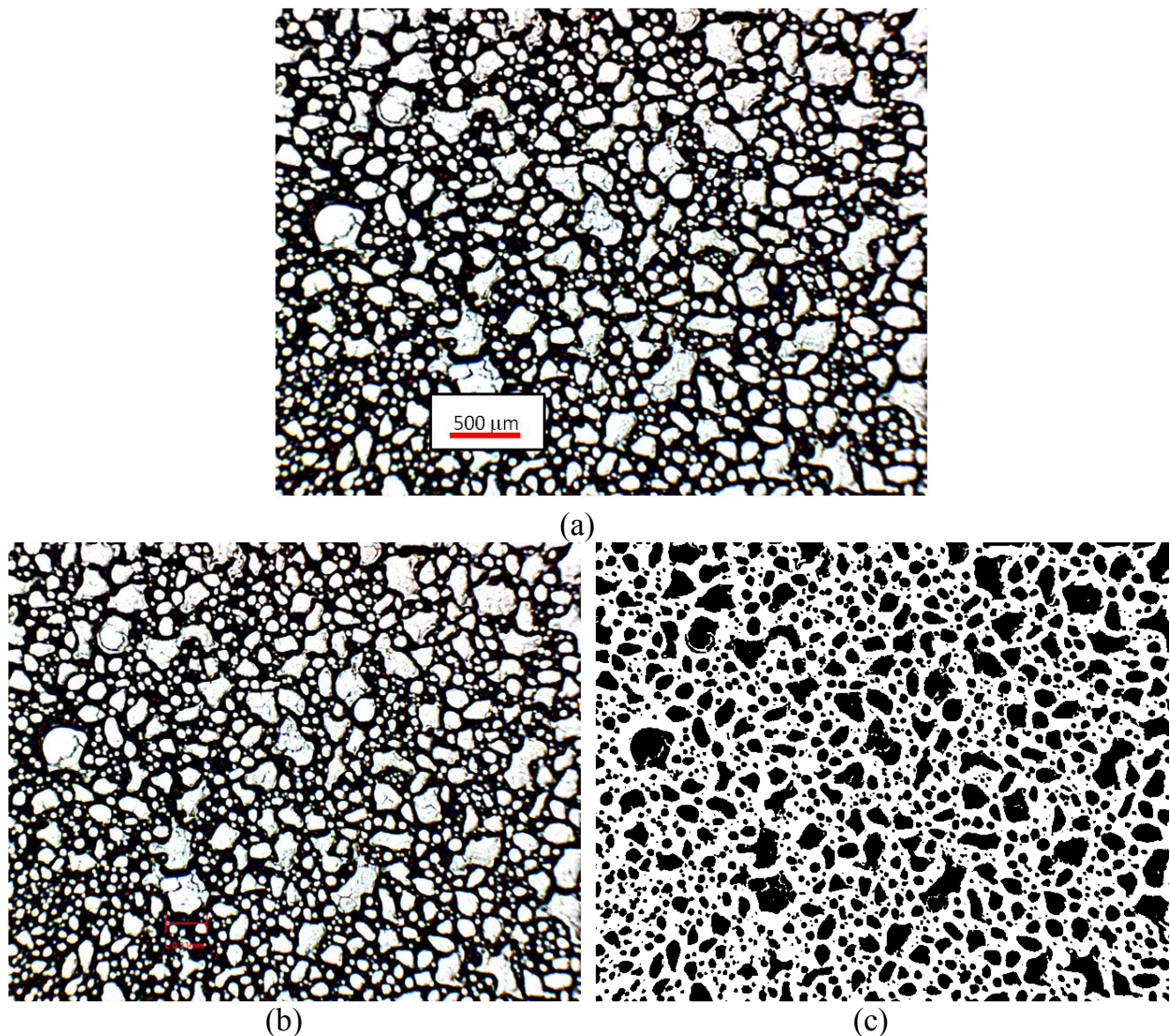
(a)

(b)

(c)

Figure 2: Result of the segmentation proposed. (a) Original image. (b) Image result of applying opening Top Hat Transform. (c) Binary image.

For every sample, several images were taken and made an average of the results. Figure 4(c) and (d) show the histograms corresponding to the size granulometric labeled images of both samples. Figure 4(e) and (f) show the corresponding histograms of the size distribution of both samples. As it can be seen, the particles made with the sol without aging (58S_TT) show an exponential probability distribution function while the 58S_AG_TT are distributed as a Poisson function. Besides, from the normalized histograms, the mean area can be calculated for both kind of images. It can be seen that the mean area of the 58S_AG_TT particles increases respect to the mean area of the no aged ones: the percentage of covered area is 48% for the samples 58S_AG_TT and 25% for the 58S_TT.

Due to the spherical shape of the deposited particles, for this work it was proposed the use the "roundness" descriptor in order to discriminate between the different type of particles discriminating their shape.

Figure 4(g) and 4(h) show the corresponding histogram of the roundness descriptor, for the 58S_TT and for the 58S_AG_TT particles onto the hybrid coating. As it can be seen when the roundness descriptor is close to one, the particle is nearly a perfect circle. For the 58S_TT sample, the greater value of frequency of the roundness factor is nearly one, which means most of the particles have a nearly circular shape, event that do not happen for the 58S_AG_TT sample.

Table 3: Individual bands and the corresponding vibrational position in the Raman spectra of the different types of sol gel glass studied. (L) is low intensity.

	58S	58S_AG	58S_TT	58S_AG_TT	$Ca(NO_3)·4H_2O$
	319(L)				
Si-O-Si	324(L)				
Si-$(OSi)_3$-OR	483(L)				
NO_3	718(fit)*	714(L)	718(L)	714(L)	713(L)
NO_3					748(L)
Si-$(OSi)_3$-OR	740(fit)*	741(L)	743(L)	742(L)	
-PO_4	820(L)	960	968(L)	967(L)	
NO_3	1051	1051	1052	1052	1051
Ca/NO_3	1059				
P-O		1087		1087	
C-O	1101	1102			
P=O	1294(L)				

* Band fitted with Origin Lab7.0 in order to determine the peaks present
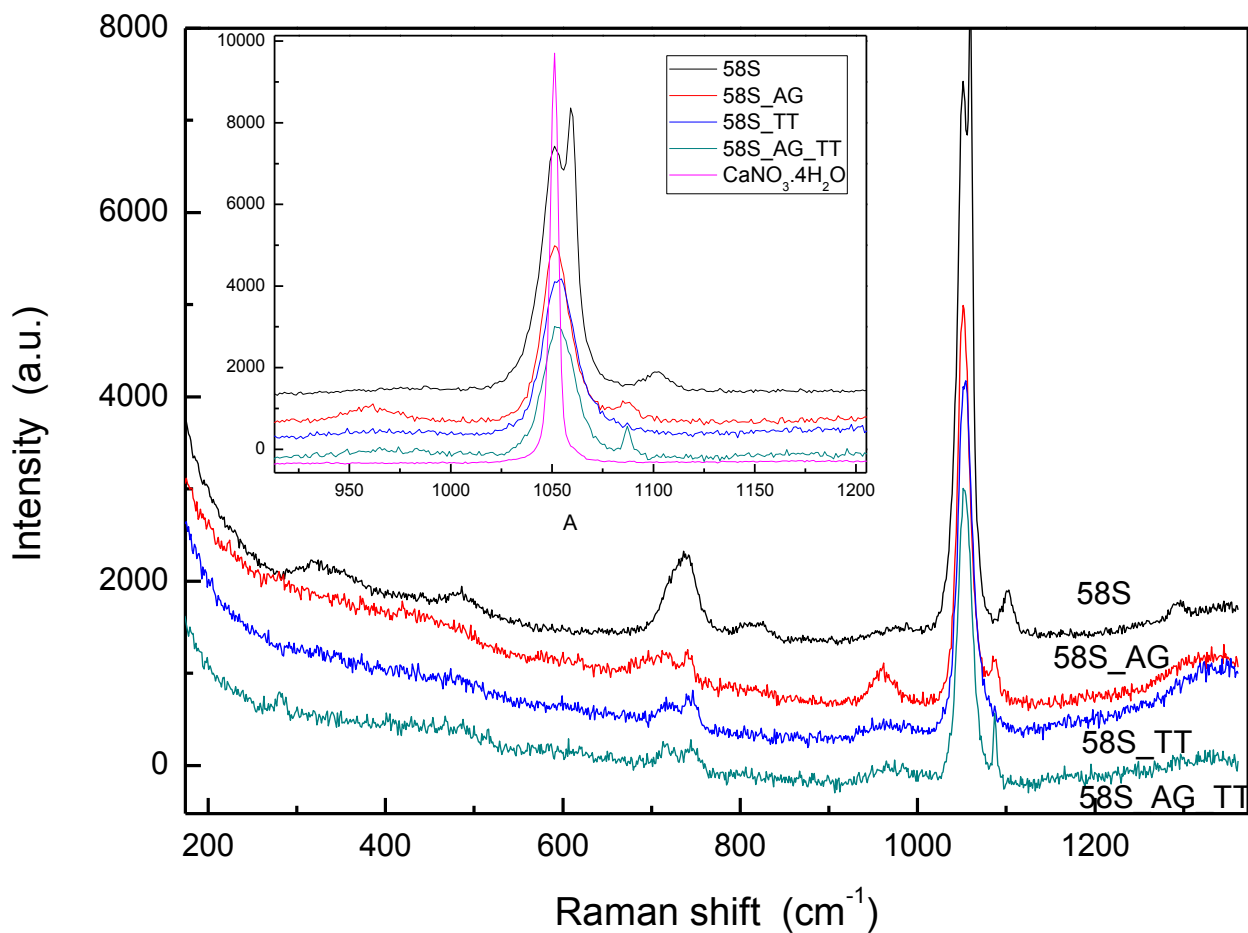

Figure 3: Raman spectra of the sol gel made glass without aging (58S and 58S_TT) and with 24 h aging (58S_AG and 58S_AG_TT). Insert, zoom-in near the nitrates band (1050 cm^{-1}) and comparing with the $CaNO_3$ used in the glass synthesis.

4 Discussion

In 1991, the incorporation of sol gel chemistry gave rise to a new generation of bioactive glasses [14]. The synthesis
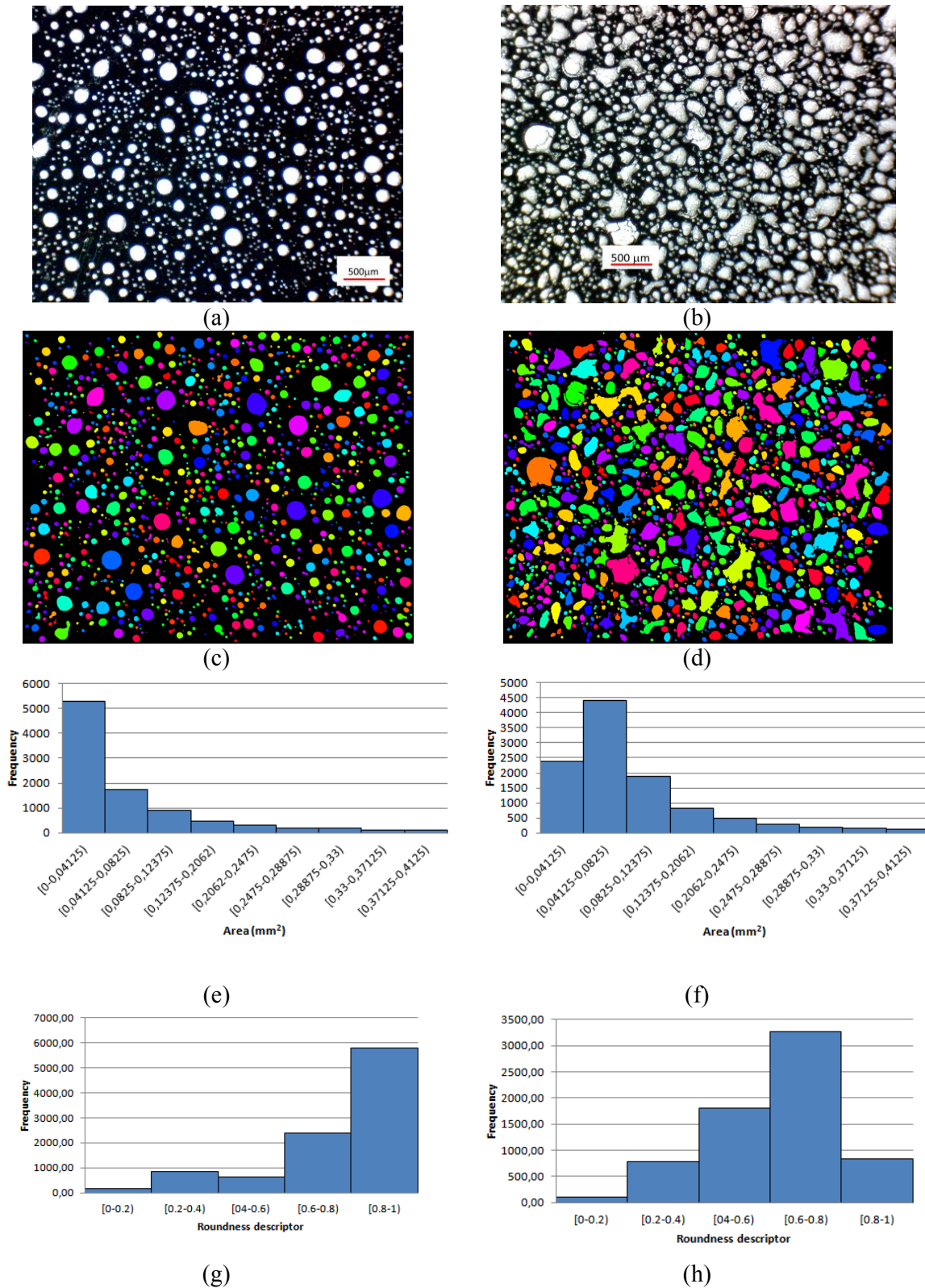
Figure 4: Stainless steel coated and with different particles deposited by spray technique: (a) 58S_TT optical image, (b) 58S_AG_TT optical image, (c) Size granulometric labeled 58S_TT optical image. (d) Size granulometric labeled 58S_AG_TT optical image, (e) histogram of the size distribution of the 58S_TT particles, (f) histogram of the size distribution of the 58S_AG_TT particles, (g) histogram of the roundness descriptor of the 58S_TT particles, and (h) histogram of the roundness descriptor of the 58S_AG_TT particles.

of a silica based glass by sol-gel generates a method that has a great potential to develop better implants or to enhance the existing ones, for bone applications. This effect can be attributed to the enhancing of the surface area and porosity derived of the sol gel processing, compared with the melting and quenching techniques used for the synthesis of conventional glasses [7].

The sol gel synthesis is simple, clean, can be made at room temperature, and fast. The time required to age and sinter the gel is short compared with other thermal treatments applied to sol gel glasses [15, 16].

The final aspect of the sol obtained in this work was clear and translucent, with no precipitates. The viscosity for the sol without ageing treatment was near 1 mPa·s, similar to water, and it lightly rises after 24 h of storage at room temperature, but it is still a solution, it does not generate a gel [17]. In this time, it is thought that the policondensation and evaporation of the solvents (water and ethanol) is taking place, and the open structure is becomimg more closed, creating higher amount of O-Si-O bonds [1]. It is expected that the ageing has an effect in particle formation and, after time, particle dissolution in soaking experiments.

To analyze the effect of thermal treatment to the gel-glass evolution, Raman spectroscopy essays were made. The 58S glass shows characteristic bands related with a silica gel doped with phosphorus made by TEOS and TEP [18], were some silanol double bonds are already present, showing that the gel is still hydrolyzing and policondensating. The effect of calcium nitrate addition can be analyzed by the 1051 cm^{-1} band. This is the more intense band related to the vibration frequency of NO^{3-} ions [19]. The presence of a 1059 cm^{-1} band can be associated with the presence of NO^{3-} coordinated with calcium cations [20]. It is clear to appreciate that when there are no ageing and thermal treatment, there are two well defined peaks at 1051 and 1059 cm^{-1}. The second band indicates that the calcium nitrate incorporated to the sol is still outside the glassy net structure. The nitrate ions are close to the calcium ions, maybe some of them even in crystalline arrange. The way of the Ca ions to enter in the silica network is by thermal migration (above $350°C$) [16], and the remaining nitrates are expected to be eliminated by the thermal treatment. As the thermal treatment chosen was $450°C$ and then, not enough to eliminate all the nitrates in the glass structure, the quantification of the 1051–52 cm^{-1} band results useful. The intensity of the principal nitrate vibrational band decreases from 5906 for the 58S glass to 3115 arbitrary units of the 58S_AG_TT glass system. The effect of ageing is slightly noticed: the presence of phosphorous entering to the structure can be denoted by the pres-

ence of 960 and 1087 cm^{-1} [18], vibrational bands related with calcium phosphates.

One of the most important item of any automated system of vision is the task of understanding the image, which severely affects the subsequent process of interpretation of the image, providing useful structures such as regions and edges [21]. The image processing techniques enabled precise and automatic particle quantification. The advantage is that the morphological granulometry allows to reproduce the results eliminating discrepancies, leading to a correct particle characterization. From the histograms corresponding to the samples 58S_TT and the 58S_AG_TT, it is clear to see that a larger number of small particles are present in the non aged sample with respect to the aged one. The degree of sphericity or ball-like shape can also be described mathematically, by the so called roundness descriptor. When the roundness descriptor is one, it means the particle is perfectly circular. Comparing both distributions (aged and not aged particles deposited on the coated substrates) it is evident that the particles are less circular after the aging treatment. This fact can be related with the solvent content and the degree of hydrolysis and poly-condensation reached after the 24 h aging: the 58S_TT particles were applied from a sol with more content of ethanol and the short term order degree of the glass structure is smaller than for the 58S_AG_TT ones, that are more "dense" or compact since the poly-condensation is more advanced [1]. It leads to more spherical particles with an open structure and more water and ethanol solvent content, and cracked and irregular shaped 58S_AG_TT particles, with a more organized and closed structure, susceptible to fracture propagation and to break. The absence of solvent does not contribute to enhance the superficial tension of the particles, and the shape starts to get away from sphericity.

Summarizing, glass particles from the system SiO_2-CaO-P_2O_5 (58S) were synthesized by simple and clean sol-gel technique, generating an open glass structure that could help to particle dissolution and apatite deposition for biological purposes. The rate of dissolution was delayed since an aging treatment was done to the sol prior to particle deposition. The particles were deposited onto a surgical grade stainless steel protected by a sol-gel hybrid organic inorganic layer, by spray technique. This deposition tool helps to have a distribution of the glass particles. A cover surface of almost 50% with the particles made with a glass aged for 24 h prior to deposition was obtained. When no aged glass particles were deposited, the particle size distribution shows the presence of many big particles with a roundness factor between 0.8 and 1 in a high percentage, meaning that they are spherical due to the pres-

ence of solvent and with a more open glass structure in the no aged glass. The Digital Image Processing and Raman spectroscopy tools help to analyze, characterize and quantify the bioactive particles deposited onto coated surgical grade stainless steel in terms of morphology, distribution and composition.

References

[1] Brinker C.J., Hurd A.J., Schunk P.R., Frye G.C., Ashley C.S., Review of sol-gel thin film formation. Journal of Non-Crystalline Solids, 1992, 147–148, 424–36.

[2] Guglielmi M., Rivestimenti sottili mediante dip coating con metodo sol-gel. Revista della Staz Sper, 1988, 4, 197–9.

[3] Sanchez C., In M. Molecular design of alkoxide precursors for the synthesis of hybrid organic-inorganic gels. Journal of Non-Crystalline Solids, 1992, 147–148, 1–12.

[4] de Sanctis O., Gomez L., Pellegri N., Parodi C., Marajofsky A., Duran A., Protective glass coatings on metallic substrates. Journal of Non-Crystalline Solids, 1990, 121, 338–43.

[5] Pellegri N., Sanctis O., Durán A., Preparation and microstructure study of borosilicate coatings produced by sol-gel. Journal of Sol-Gel Science and Technology, 1994, 2, 519–23.

[6] Rámila A., Balas F., Vallet-Regí M., Synthesis routes for bioactive sol-gel glasses: Alkoxides versus nitrates. Chemistry of Materials, 2002, 14, 542–8.

[7] Izquierdo-Barba I., Salinas A.J., Vallet-Regí M., Bioactive Glasses: From Macro to Nano. International Journal of Applied Glass Science, 2013, 4, 149–61.

[8] Jones J.R., Review of bioactive glass: From Hench to hybrids. Acta Biomaterialia, 2013, 9, 4457–86.

[9] Ronse C., Heijmans H.J.A.M., The algebraic basis of mathematical morphology. II. Openings and closings. CVGIP: Image Understanding, 1991, 54, 74–97.

[10] Serra J., Image Analysis and Mathematical Morphology, 1982, vol I.

[11] Serra J., Image analysis and mathematical morphology, 1988, vol II.

[12] Otsu N., A threshold selection method from gray level histogram. IEEE Trans Syst Man Cybern, 1979, *9*.

[13] Rothe I., Susse H., Voss K., The method of Normalization to determine invariants. IEEE Transactions on Pattern Analysis and Machine Intelligence, 1996, vol 18.

[14] Li R., Clark A.E., Hench L.L., An investigation of bioactive glass powders by sol-gel processing. Journal of Applied Biomaterials, 1991, 2, 231–9.

[15] Saboori A., Sheikhi M., Moztarzadeh F., Rabiee M., Hesaraki S., Tahriri M., *et al.*, Sol-gel preparation, characterisation and in vitro bioactivity of Mg containing bioactive glass. Advances in Applied Ceramics, 2009, 108, 155–61.

[16] Martin R.A., Yue S., Hanna J.V., Lee P.D., Newport R.J., Smith M.E., *et al.*, Characterizing the hierarchical structures of bioactive sol-gel silicate glass and hybrid scaffolds for bone regeneration. Philosophical Transactions of the Royal Society A: Mathematical, Physical and Engineering Sciences, 2012, 370, 1422–43.

[17] Hesaraki S., Alizadeh M., Nazarian H., Sharifi D., Physicochemical and in vitro biological evaluation of strontium/calcium silicophosphate glass. Journal of Materials Science: Materials in Medicine, 2010, 21, 695–705.

[18] Todan L., Anghel E.M., Osiceanu P., Turcu R.V.F., Atkinson I., Simon S., *et al.*, Structural characterization of some sol-gel derived phosphosilicate glasses. Journal of Molecular Structure, 2015, 1086, 161–71.

[19] Kondilenko I.I., Korotkov P.A., Golubeva N.G., Effect of water of crystallization on spontaneous Raman spectrum of calcium and magnesium nitrates. Journal of Applied Spectroscopy, 1975, 20, 775–9.

[20] Naumov V.S., Study of sodium interaction with calcium nitrate and carbonate in alkali metal chloride melts by IR and raman spectroscopy. Russian Journal of Inorganic Chemistry, 2010, 55, 1202–8.

[21] Gonzalez R., Woods R., Digital Image Processing, 1992.